JACS
JOURNAL OF THE AMERICAN CHEMICAL SOCIETY
Article
pubs.acs.org/JACS

The Elusive Structure of $Pd_2(dba)_3$. Examination by Isotopic Labeling, NMR Spectroscopy, and X-ray Diffraction Analysis: Synthesis and Characterization of $Pd_2(dba\text{-}Z)_3$ Complexes

Anant R. Kapdi,[†] Adrian C. Whitwood, David C. Williamson, Jason M. Lynam, Michael J. Burns, Thomas J. Williams, Alan J. Reay, Jordan Holmes, and Ian J. S. Fairlamb*

Department of Chemistry, University of York, Heslington, York, North Yorkshire, YO10 5DD, United Kingdom

Supporting Information

ABSTRACT: $Pd^0_2(dba)_3$ (dba = *E,E*-dibenzylidene acetone) is the most widely used Pd^0 source in Pd-mediated transformations. $Pd^0_2(dba\text{-}Z)_3$ (Z = dba aryl substituents) complexes exhibit remarkable and differential catalytic performance in an eclectic array of cross-coupling reactions. The precise structure of these types of complexes has been confounding, since early studies in 1970s to the present day. In this study the solution and solid-state structures of $Pd^0_2(dba)_3$ and $Pd^0_2(dba\text{-}Z)_3$ have been determined. Isotopic labeling (^2H and ^{13}C) has allowed the solution structures of the freely exchanging major and minor isomers of $Pd^0_2(dba)_3$ to be determined at high field (700 MHz). DFT calculations support the experimentally determined major and minor isomeric structures, which show that the major isomer of $Pd^0_2(dba)_3$ possesses bridging dba ligands found exclusively in a *s-cis,s-trans* conformation. For the minor isomer one of the dba ligands is found exclusively in a *s-trans,s-trans* conformation. Single crystal X-ray diffraction analysis of $Pd^0_2(dba)_3{\cdot}CHCl_3$ (high-quality data) shows that all three dba ligands are found over two positions. NMR spectroscopic analysis of $Pd^0_2(dba\text{-}Z)_3$ reveals that the aryl substituent has a profound effect on the rate of Pd-olefin exchange and the global stability of the complexes in solution. Complexes containing the aryl substituents, 4-CF_3, 4-F, 4-*t*-Bu, 4-hexoxy, 4-OMe, exhibit well-resolved ^1H NMR spectra at 298 K, whereas those containing 3,5-OMe and 3,4,5-OMe exhibit broad spectra. The solid-state structures of three $Pd^0_2(dba\text{-}Z)_3$ complexes (4-F, 4-OMe, 3,5-OMe) have been determined by single crystal X-ray diffraction methods, which have been compared with Goodson's X-ray structure of $Pd^0_2(dba\text{-}4\text{-}OH)_3$.

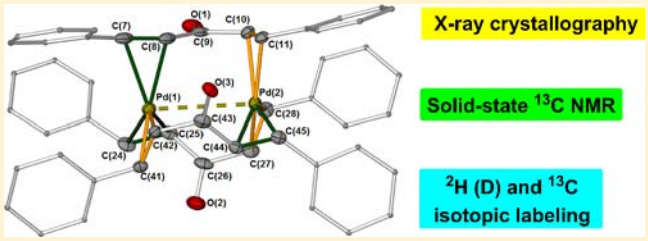

INTRODUCTION

$Pd^0_2(dba)_3$ is the most widely used Pd^0 precursor complex in synthesis and catalysis.[1] Since early studies in the 1970s, determination of the precise structure of $Pd^0_2(dba)_3$ has proven confounding *vide infra*. Dba acts as an olefin, enone,[2] or 1,4-dien-3-one ligand and is often noninnocent[3] (i.e., involved in key steps) in catalytic processes.[4] $[Pd^0(\eta^2\text{-dba})L_n]$ (L = phosphine or *N*-heterocyclic carbene) complexes are formed in catalytic processes, generated by addition of ligand to $Pd^0_2(dba)_3$ *in situ*;[5] dba-ligation affects the concentration of Pd^0L_n species available for oxidative addition with organohalides, the first committed step in cross-coupling processes, and can act positively in regulating the concentration of Pd^0L_n when reactive organohalides are used (e.g., ArI) and reduce Pd agglomeration which can form large inactive Pd^0 clusters.[6] Recent selected examples where $Pd^0_2(dba)_3$ has been employed as a powerful catalyst system are given in Scheme 1, which range from a remarkable macrocyclization,[7] N^1-selective arylation of unsymmetrical imidazoles,[8] and a highly selective polycondensation process.[9]

By electronically tuning the aryl groups of dba (e.g., dba-Z,[10] where Z = OMe, *t*-Bu, H, F, CF_3), the noninnocent behavior has been exploited experimentally in several cross-coupling processes,[11] and their effects supported by theoretical studies.[12] The dba-Z ligands also influence transmetalation and reductive elimination steps[13] and reduce the rate of β-hydrogen elimination in "Pd^{II}-σ-alkyl" complexes.[14] This latter finding facilitates intramolecular Heck reactions of alkenyl tethered alkyl bromides to give *exo*-cyclopentene products (providing dba-4-OMe is used). Furthermore, dba-4-Z (Z = CF_3 or OMe) ligands influence regiochemical effects in the cross-coupling of aryl halides with allylic sililoate salts.[15] The design of dba-structures incorporating thienyl (th) rings affords $Pd^0_2(th\text{-}dba)_3$ complexes, allowing oxidative addition rates to be controlled.[16] $Pd_2(dba\text{-}4\text{-}OH)_3$ and $Pd_2(dba\text{-}4\text{-}OAc)_3$ complexes have been adapted for use in aqueous Suzuki polycondensation reactions.[17]

In this paper we detail the synthesis and characterization of several Pd^0 complexes containing symmetrical aryl-substituted 'dba-Z' ligands. In order to achieve this task it has been necessary to study the solution and solid-state structures of the parent complex, $Pd^0_2(dba)_3$, and unambiguously determine its structure by use of isotopic labeling (^2H and ^{13}C). The solid-

Received: April 5, 2013
Published: May 23, 2013

   dx.doi.org/10.1021/ja403259c | *J. Am. Chem. Soc.* 2013, 135, 8388−8399

Scheme 1. Powerful $Pd_2(dba)_3$-Mediated Coupling Processes

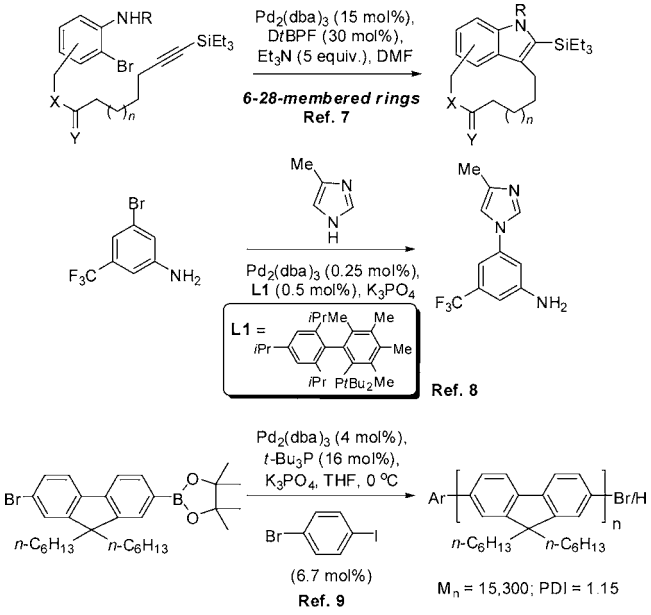

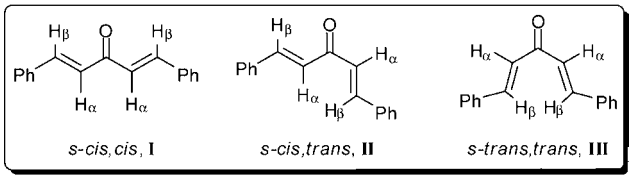

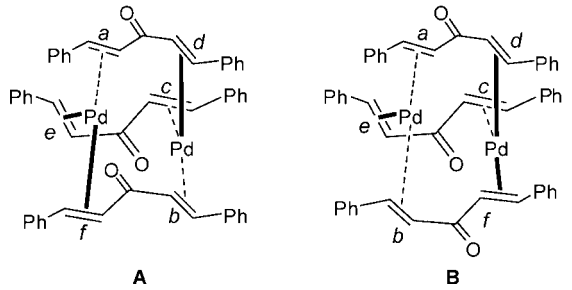

Figure 1. Three conformations for dba (**I**–**III**) and the solution structure(s) of $Pd^0_2(dba)_3$. Bold lines denote strong olefin bonding interactions (f > e > d), and dashed lines denote weak olefin bonding interactions (c > b > a). (A) and (B) are the isomers proposed as most likely in the Kawazura study.

state characterization of a series of $Pd_2(dba\text{-}Z)_3{\cdot}CH_2Cl_2$ complexes (Z = 3,5-OMe, 4-OMe, and 4-F) has been conducted by X-ray diffraction. The study is placed into context with that reported for $Pd_2(dba\text{-}4\text{-}OH)_3$,[17] specifically the importance associated with intermolecular H-bonding stabilizing one isomeric form (with no apparent conformational disorder) of the dba-backbone in the dinuclear Pd^0 complexes. For several $Pd_n(dba\text{-}Z)_{n+1}$ complexes it has been possible to probe their solution behavior and stability, by ^1H NMR spectroscopy, which is comparable to the spectroscopic data for $Pd_2(dba)_3$.

RESULTS AND DISCUSSION

Structure of $Pd^0_2(dba)_3$ in $CDCl_3$ and Additional Context. In 1978 the solution behavior of $Pd^0_2(dba)_3{\cdot}CHCl_3$ [hereafter '$Pd^0_2(dba)_3$' unless reference is made to an alternative solvate] was valiantly investigated by Kawazura and co-workers[18] by a combination of ^1H NMR spectroscopy (at 100 MHz), ^2H labeling, and computational simulation. This work showed that each olefin in $Pd^0_2(dba)_3$ can be found in a distinct chemical environment. That is six olefins coordinate to two chemically unique Pd^0 atoms, with each dba acting as a "η^2-olefin,η^2-olefin" bridging ligand. To explain why six olefins are observed spectroscopically one needs to consider that: (i) dba can exist in one of three 1,4-dien-3-one conformations (**I**–**III**, Figure 1); (ii) the preferred conformation for dba in binding Pd^0 in the dinuclear complex, $Pd_2(dba)_3$, being *s-cis,s-trans* (**II**); and (iii) the strength of the η^2-olefin-metal bonding interactions, via coordination through *s-cis* and *s-trans* olefins, is different; the proposed solution-state structure of '$Pd_2(dba)_3$' (one of two possible isomers) is shown in Figure 1.

The Kawazura study[18] relied on two pieces of information: (i) NOE proton contacts between neighboring olefins within two of the three coordinating dba ligands; and (ii) the chemical shift difference between α- and β-protons within individual olefins ($\Delta\alpha\beta = \delta\beta - \alpha$). This latter information can provide an indication of the enone conformation in dba.[19] For example in the noncoordinated dba the *s-cis* form has a minimum $\Delta\alpha\beta$ value of 0.5 ppm and in the *s-trans* form a maximum value of 1.5 ppm.

Deformation toward the *s*-skew form causes $\Delta\alpha\beta$ to increase for the *s-cis* conformer, whereas it decreases for the *s-trans* conformer. By extrapolation coordinated olefins with a small $\Delta\alpha\beta$ value (δ 0.069–0.186 ppm) were proposed to be in the *s-cis* form, whereas those with a large value (δ 0.631–0.965 ppm) were in a *s-trans* form. However, our recent work[20] on 'dba-coordinated' metal complexes (Rh, Pd, Pt, and Cu)[21] show that these ranges are underestimated, leaving the structural connectivity reliant on NOE contacts and a low-resolution ^1H NMR spectrum. It is clear that there are few structures containing palladium that are more spectroscopically confounding than '$Pd^0_2(dba)_3$'.

In a study reported in 2012, Zalesskiy and Ananikov reported[22] high-field (600 MHz) NMR spectroscopic data for '$Pd^0_2(dba)_3$' as a mixture of two isomers—the first time a second 'minor' isomer was reported in solution.[23] Through a combination of COSY, LR-COSY, HSQC, HMBC, and NOESY measurements, the authors proposed that the dba ligands in $Pd_2(dba)_3$ were in fact found in a *s-cis,s-cis* conformation, standing in stark contrast with the Kawazura study. ^1H DOSY measurements confirmed that the major and minor isomeric species had identical diffusion coefficients, i.e., two forms of $Pd^0_2(dba)_3$. Following on from work on $Pd^0_2(dba\text{-}Z)_3$ complexes, we were aware of their intricate solution NMR spectra (see later), due to their inherent low symmetry, dba-Z lability, and inter- and intramolecular exchange. On symmetry reasons alone it seemed unlikely that a *s-cis,s-cis* conformation would be preferred, i.e., on the NMR time scale all three ligands and associated olefins (six) would be expected to bind Pd^0 to the same extent, e.g., as averaged signals with only two α- and β-proton environments, which is not the case (free exchange occurs at ca. 298 K). The *s-cis,s-cis* conformations were discounted for these reasons in the Kawazura study.[18] Given these details, an independent high-field NMR spectroscopic study on the structure of $Pd^0_2(dba)_3$ in solution ($CDCl_3$) was conducted. We selected $Pd^0_2(dba)_3{\cdot}$dba as from experience some free dba ligand is observed spectroscopically in solutions

dx.doi.org/10.1021/ja403259c | J. Am. Chem. Soc. 2013, 135, 8388–8399

of $Pd^0_2(dba)_3$·solvent (solvent = $CHCl_3$, CH_2Cl_2, or benzene). At this point it is worth noting that $Pd^0_2(dba)_3$ is potentially sensitive in solution to photooxidation [λ_{max} = 520 nm (MLCT) in $CHCl_3$],[24] in addition to thermal degradation. A ^{1}H NMR spectrum (700 MHz) of $Pd^0_2(dba)_3$·dba [hereafter $Pd^0_2(dba)_3$] in alumina-filtered $CDCl_3$ reveals the Pd^0-olefin bonding interactions (Figure 2).

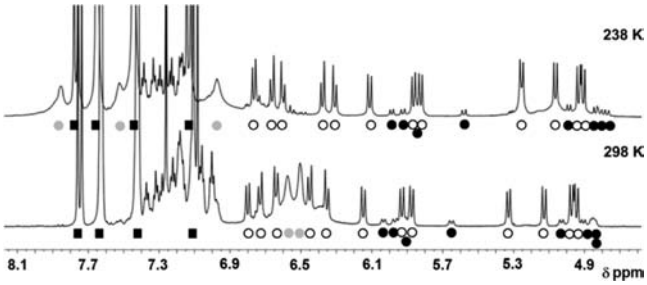

Figure 2. 700 MHz ^{1}H NMR spectra of $Pd^0_2(dba)_3$·dba at 298 K (bottom) and 238 K (top) (in $CDCl_3$, referenced to residual $CHCl_3$ at δ 7.26). Key: closed black square, free dba; closed gray circle, *ortho*-aryl protons; open circles, olefin protons in major species; closed black circles, olefin protons in minor species.

Free dba ligand is observed in the ^{1}H NMR spectrum (highlighted by black squares). Proton integration reveals the stoichiometry as $Pd^0_2(dba)_3$·dba (in agreement with the C,H composition indicated by elemental analysis). Two broad signals, indicative of an exchange process, are observed at ca. δ 6.35−6.65 ppm which are the shielded *ortho*-protons of the aromatic groups (ca. 12 H) connecting the 1,4-dienone moieties of three dba ligands in $Pd^0_2(dba)_3$ (indicated by gray circles). These broad signals overlap with resolved olefin protons in the same chemical shift region (at 298 K). Cooling this solution to 238 K, where negligible inter- or intramolecular exchange occurs (established by EXSY experiments), resulted in the broad aromatic protons shifting to higher chemical shift (three broad signals at ca. δ 7.0, 7.55 and 7.85), leaving 12 resolved Pd^0-olefin protons signals.

The three dba ligands thus bridge two Pd^0 atoms in an unsymmetrical manner, e.g., "η^2-olefin,η^2-olefin", involving the coordination of six independent alkenes, i.e., three distinct dba ligands. Shown by open circles are the olefin protons attributed to six unique olefins in $Pd^0_2(dba)_3$. In both spectra run at 298 and 238 K, a minor species was also observed, akin to that reported by Zalesskiy and Ananikov.[22] Highlighted by black circles are eight olefin protons (Figure 2), which belong to the minor species (ratio of major/minor isomeric species 1:0.23 at 298 K).

The connectivity of each alkene in both major and minor isomers needed to be confirmed by a combination of NMR experiments and isotopic labeling (deuterium and ^{13}C; Figures 3 and 4). The latter was necessary to ascertain the position of the α- and β-protons, which could allow each olefin to be located accurately. The isotopically labeled dba ligands and Pd^0 complexes were prepared in an identical manner to $Pd^0_2(dba)_3$

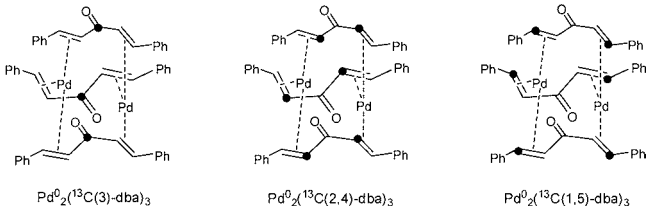

Figure 4. ^{13}C Isotopically labeled $Pd^0_2(dba)_3$ complexes synthesized for this study (black circle indicates the position of ^{13}C).

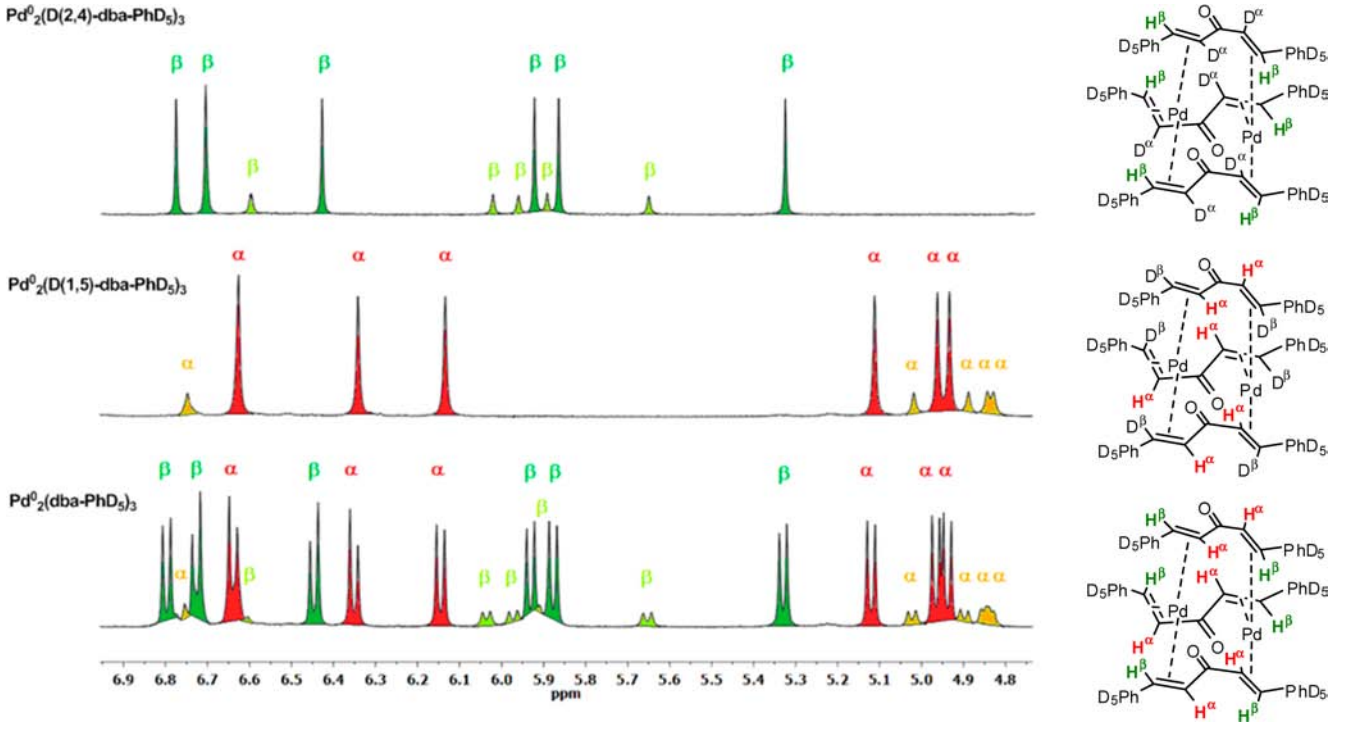

Figure 3. 700 MHz ^{1}H NMR spectra (at 298 K) of $Pd^0_2(D(2,4)\text{-dba-PhD}_5)_3$, $Pd^0_2(D(1,5)\text{-dba-PhD}_5)_3$, and $Pd^0_2(\text{dba-PhD}_5)_3$ (red and green colors used to depict the α- and β-protons in the major isomer). Note that ^{1}H−^{2}H spin−spin couplings are not observed in these spectra.

dx.doi.org/10.1021/ja403259c | J. Am. Chem. Soc. 2013, 135, 8388−8399

on small scale (typically 100 mg) (Figure 4). The ^{1}H NMR spectra of the deuterium-labeled Pd^0 complexes are shown in Figure 3.

Considering the major isomer then, the ^{1}H NMR spectrum for Pd$^0_2$(dba-PhD$_5$)$_3$ shows the α-protons (red) and β-protons (green), which were located by comparison with the spectra of Pd$^0_2$(D(1,5)-dba-PhD$_5$)$_3$ and Pd$^0_2$(D(2,4)-dba-PhD$_5$)$_3$. The protons do not exhibit spin−spin coupling to deuterium due to exchange at 298 K (in combination with small quadrupolar effects). The spectra for Pd$^0_2$(D(2,4)-dba-PhD$_5$)$_3$ and Pd$^0_2$(D-(1,5)-dba-PhD$_5$)$_3$ also reveal additional minor isomeric proton signals, shown in light green for the former complex and orange for the latter complex. These isomers were overlapping with the major species in the spectrum of Pd$^0_2$(dba-PhD$_5$)$_3$ [and unlabeled Pd$^0_2$(dba)$_3$].

As the ^{2}H labeling had been successful in locating the α- and β-protons in the major isomer of Pd$^0_2$(dba)$_3$ (and most of them in the minor isomer), we anticipated that ^{13}C labeling would provide valuable ^{13}C NMR spectroscopic data; due to the limited solubility of Pd$^0_2$(dba)$_3$ in CDCl$_3$ (ca. 5 mg/mL) it was deemed necessary to synthesize ^{13}C labeled analogues. The ^{13}C{^{1}H} NMR spectra of Pd$^0_2$(^{13}C(3)-dba)$_3$, Pd$^0_2$(^{13}C(2,4)-dba)$_3$, and Pd$^0_2$(^{13}C(1,5)-dba)$_3$ are shown in Figure 5, and the spectroscopic data is collated in Table 1. ^{13}C labeling shows the positions of all the ^{13}C nuclei within the 1,4-dien-3-one backbone of the three dba ligands, in both major and minor isomers, and also reveals valuable ^{13}C−^{13}C spin−spin coupling information, e.g., in Pd$^0_2$(^{13}C(2,4)-dba)$_3$.

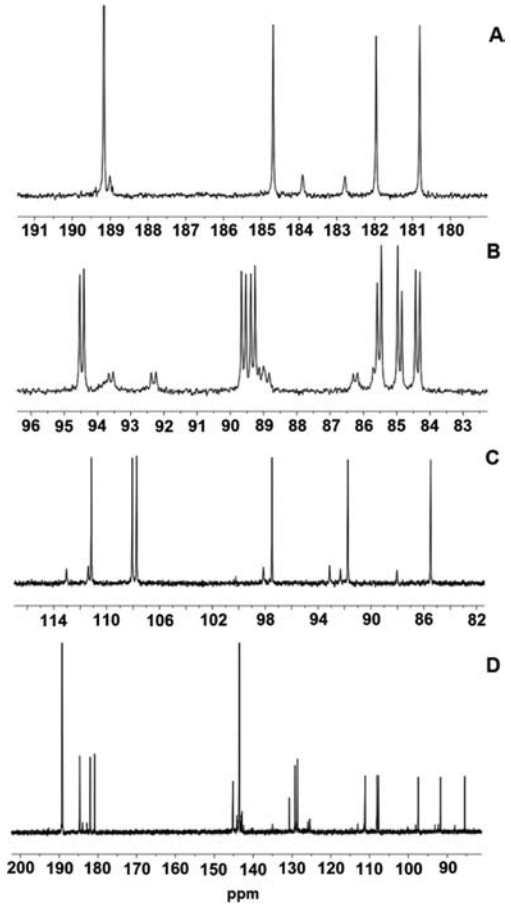

Figure 5. ^{13}C{^{1}H} NMR spectra (at 300 K, 125 MHz) of: (A) Pd$^0_2$(^{13}C(3)-dba)$_3$; (B) Pd$^0_2$(^{13}C(2,4)-dba)$_3$; (C) Pd$^0_2$(^{13}C(1,5)-dba)$_3$; (D) ^{13}C{^{1}H} NMR spectrum following addition of 1 equiv of ^{13}C(1,5)-dba to a CDCl$_3$ solution of Pd$^0_2$(^{13}C(3)-dba)$_3$.

For the major and minor species of Pd$^0_2$(dba)$_3$ there are six independent olefins, confirming their isomeric relationship. In the major isomer the carbonyl moieties [located from Pd$^0_2$(^{13}C(3)-dba)$_3$] are all found in different chemical environments and shifted between δ 4.5−8.4 from the free dba ligand (δ 189.2). The minor isomer exhibits a similar coordination shift for two of the three dba ligands (δ 5.3 and 6.4). However, the remaining C═O signal exhibits a shift of only δ 0.2, which is very close to the free ligand. This latter signal could belong to a dba contaminant, rather than the minor isomer, leaving the remaining dba C═O overlapping with the major isomer of the Pd$^0_2$(^{13}C(3)-dba)$_3$.

The α-carbons (six) in the major isomer are in different chemical environments shifted to δ 84.4−94.5, and $^2J_{CC}$ coupling is observed between olefins within the same dba ligand. Three α-carbons can be grouped δ 84.4−85.5 and the remaining α-carbons δ 89.3−94.5. The magnitude of the coupling across the six α-carbons is 15.8−16.2 Hz (±0.1 Hz). Similar carbon signals are seen for the minor isomer; indeed the average coordination shifts from the free ligand are similar in both major and minor isomers (37.6 and 36.4 ppm, respectively). The coordination shift difference between the lowest and highest chemical shift signals was 10.1 and 8.0, for the major and minor isomers, respectively.

The β-carbons (six) in the major isomer are also in different chemical environments shifted to δ 85.5−111.2. Three β-carbons can be grouped δ 85.5−97.5 and the remaining β-carbons δ 107.7−111.2. Four β-carbon signals for the minor isomer can be grouped δ 88.0−98.1, with the remaining β-carbons δ 111.4−113.0. The average coordination shifts from the free ligand are similar in both major and minor isomers (43.3 and 44.3 ppm, respectively). The coordination shift difference between the lowest and highest chemical shift signals was 25.7 and 25.0 ppm for the major and minor isomers, respectively. Interestingly, four of the β-carbon signals in the minor isomer have a coordination shift >45 ppm, whereas only three of the β-carbon signals are >45 ppm in the major isomer. It is clear from these ^{13}C NMR spectra that the β-carbons are more responsive to coordination to Pd^0 than the α-carbons. EXSY experiments on this isotopically labeled derivative show that the exchange mechanism is complex (see SI for spectra). Spectrum D (Figure 5) shows the rapid exchange of added ^{13}C(1,5)-dba to Pd$^0_2$(^{13}C(3)-dba)$_3$ (in CDCl$_3$).

In keeping with the Kawazura study three of the olefins (H1 through to H6) are involved in strong binding to Pd^0 (denoted by 'S' in Table 1), and three olefins (H7−H12) are involved in weak binding (denoted by 'W' in Table 1). This was originally proposed by considering the average olefin chemical shifts.[18] It is noticeable that all the S olefins are found in a *s-trans* conformation with respect to the carbonyl group, whereas W olefins are found in a *s-cis* conformation. Thus, the 'S' olefins have average chemical shifts of δ 5.18 (olefin f), 5.45 (olefin e), and δ 5.56 (olefin d) and 'W' olefins δ 6.43 (olefin c), δ 6.51 (olefin b), and δ 6.72 (olefin a). A ^{13}C−COSY experiment confirmed the connection of α-carbons ($^2J_{CC}$ coupled), which along with ^{1}H−^{13}C HSQC experiments (see SI) allowed all the α- and β-carbons to be connected to their respective protons.

$^1J_{CH}$ couplings (ca. 157−160 Hz) are observed in ^{1}H NMR spectra of both Pd$^0_2$(^{13}C(2,4)-dba)$_3$ and Pd$^0_2$(^{13}C(1,5)-dba)$_3$, although no change in the magnitude of coupling as a function of chemical environment was recorded.

dx.doi.org/10.1021/ja403259c | J. Am. Chem. Soc. 2013, 135, 8388−8399

Table 1. Combined ^{1}H and ^{13}C NMR Spectroscopic Data for the Major Isomer of $Pd^0_2(dba)_3$ in $CDCl_3$

olefin[a]	δ_α/ppm[b]	δ_β/ppm[b]	$\delta_{\beta-\alpha}$/ppm[c]	$\delta_{ave\ \alpha\beta}$[d]	J/Hz[e]	NOE[f]	olefin binding strength[g]	HMQC[h]	conformer/olefin (a–f)/dba (**I**–**III**)[i]
H1–H5	4.9 (H1)	5.9 (H5)	1.0	5.45	12.7 $^3J_{H1-H5}$	H5β-H8α	S	C5–H5···H1	*s-trans*, e, **I**
C1–C5	84.9 (C1)	97.5 (C5)	12.6	91.0	15.8 $^2J_{C1-C8}$				
H2–H4	5.0 (H2)	5.36 (H4)	0.36	5.18	12.4 $^3J_{H2-H4}$	H4β-H10α	S	C4–H4···H2	*s-trans*, f, **II**
C2–C4	84.4 (C2)	85.5 (C4)	1.2	84.7	16.2 $^2J_{C2-C10}$				
H3–H6	5.16 (H3)	5.96 (H6)	0.8	5.56	13.0 $^3J_{H3-H6}$	H6β-H7α	S	C6–H6···H3	*s-trans*, d, **III**
C3–C6	94.5 (C3)	91.8 (C6)	−2.7	92.9	15.8 $^2J_{C3-C7}$				
H7–H12	6.18 (H7)	6.83 (H12)	0.65	6.51	13.2 $^3J_{H7-H12}$	H7α-H6β	W	C12–H12···H7	*s-cis*, b, **III**
C7–C12	89.6 (C7)	108.1 (C12)	18.5	98.7	15.8 $^2J_{C7-C3}$				
H8–H9	6.38 (H8)	6.48 (H9)	0.1	6.43	13.2 $^3J_{H8-H9}$	H8α-H5β	W	C9–H9···H8	*s-cis*, c, **I**
C8–C9	85.5 (C8)	107.7 (C9)	22.2	96.4	15.8 $^2J_{C8-C1}$				
H10–H11	6.67 (H10)	6.76 (H11)	0.09	6.72	13.4 $^3J_{H10-H11}$	H10α-H4β	W	C11–H11···H10	*s-cis*, a, **II**
C10–C11	89.3 (C10)	111.2 (C11)	21.8	100	16.2 $^2J_{C10-C2}$				

[a]Protons numbered from the lowest chemical shift (H1) to highest chemical shift (H12). [b]Position of α- and β-protons was located from the ^{1}H and ^{13}C NMR spectra of the ^{2}H and ^{13}C labeled $Pd^0_2(dba)_3$ complexes. [c]Chemical shift difference between α- and β-protons. [d]Average chemical shift between α- and β-protons. [e]Spin–spin coupling constants determined from 1D ^{1}H and ^{13}C NMR spectra [with assistance from ^{1}H–COSY and ^{13}C-HMQC spectra (at 298 K), see SI]. [f]Determined by NOE measurements (quantitative; magnitude of NOE, ca. 10%). [g]Strength of olefin binding: for the strongest binding average ^{1}H and ^{13}C chemical shifts of α- and β-protons δ_H 5.18–5.56 (δ_C 84.7–92.9) and weakest binding δ_H 6.43–6.72 (δ_C 96.4–100). [h]The ^{1}H–^{13}C correlations were determined by an HMQC experiment with $Pd^0_2(^{13}C(1,5)\text{-dba})_3$ described as $^1J_{CH}$ and $^2J_{CH}$, e.g., $^1J_{C5H5}$ and $^1J_{C5H1}$. [i]Conformation of alkene connected to the C=O group (determined by NOE), specific olefin (from ^{1}H–COSY) lettered according to average ^{1}H and ^{13}C chemical shifts of α- and β-protons (the olefin with the weakest binding to Pd^0 is denoted 'a' and that with the strongest binding 'f'. ^{13}C–^{13}C COSY (125 MHz) correlated signals for $Pd^0_2(^{13}C(2,4)\text{-dba})_3$ are 94.5 (C3) and 89.6 (C7) (conformer **III**); 89.3 (C10) and 84.4 (C2) (conformer **II**); 85.5 (C8) and 84.9 (C1) (conformer **I**).

With the data above in hand one can employ HSQC/HMQC and NOESY experiments to fully connect the protons and carbon environments in the individual dba ligands. The full structural connectivity of the major isomer of $Pd^0_2(dba)_3$ could be essentially deduced from the ^{1}H–COSY and NOESY data of the unlabeled $Pd^0_2(dba)_3$ (at 238 K, where there is negligible inter- or intramolecular exchange) (Figure 6 and Table 1). The NOE interactions (cross-peaks) provide unequivocal proof that each ligand in the major isomer is *s-cis,s-trans*. Specifically, H5β-H8α, H4β-H10α, and H6β-H7α (summarized in Figure 7).

The spectroscopic data for the minor isomer of $Pd^0_2(dba)_3$ are collated in the SI (summarized in Figure 8). Four of the olefins (H1′ through to H8′) are involved in strong binding to Pd^0 ($\delta_{ave\ \alpha\beta}$ < 5.5 ppm), and two olefins (H9′-H12′) are involved in weak binding (detected by ^{13}C–^{1}H correlations, HMQC, having very small $\alpha\beta$ chemical shift separations).

The NOE data for the unlabeled complex allowed two of the olefins in one dba ligand to be paired, that is the β-protons H5′β and H7′β, which is therefore *s-trans,s-trans*. 2D NOESY on the $Pd^0_2(D(2,4)\text{-dba-PhD}_5)_3$ compound showed the same NOE cross-peak between the β-protons H5′ and H7′. A weak correlation is seen for H8′β with a proton at d 6.76. Due to resolution issues we could not fully deduce the proton–carbon connectivity for the minor isomer from HMQC or HSQC experiments (see SI). The ^{13}C–^{13}C COSY (125 MHz) spectrum of $Pd^0_2(^{13}C(2,4)\text{-dba})_3$ in $CDCl_3$ showed well-resolved correlated signals: 93.6 and 89.1; 92.3 and 85.6; 88.9 and 86.2.

DFT Calculations. We estimate that there are 64 potential isomers of $Pd^0_2(dba)_3$. Considering the substantial computational effort needed to determine accurate structures for all of these isomers, DFT calculations were conducted on the four most likely isomers of $Pd^0_2(dba)_3$ (Table 2). The starting point used for the calculations was Goodson's X-ray structure of $Pd^0_2(dba\text{-}4,4'\text{-}OH)_3$,[17] which shows only one isomer in the solid state (denoted isomer **M** in Table 2). Isomer **M** has the lowest relative energy (set to 0) of the four isomeric structures. Altering the conformation of one dba ligand in isomer **M**, i.e., the conformation of one enone (*s-cis* ↔ *s-trans*) gives isomers **N** and **O**. The isomer containing a *s-trans,s-trans* ligand is lower in relative energy than the isomer containing a *s-cis,s-cis* ligand. The structure containing all *s-trans* enones at Pd1 and all *s-cis* enones at Pd2 has the highest relative energy of the series. The order of relative energy (stability) is **M** < **N** < **O** ≪ **P**. Therefore, the most likely isomers, in comparison with the NMR spectroscopic data presented above, are **M** and **N**, i.e., major and minor isomers of $Pd^0_2(dba)_3$, respectively (Figure 9). It is interesting to note that the olefins occupying a *s-trans* conformation in isomers **M** and **N** are more strongly bound to Pd^0 in both isomeric structures, which is in keeping with the synergic (back-bonding) arguments that the *s-trans* olefin protons are more shielded than the *s-cis* olefins.

Single Crystal X-ray Structure of $Pd^0_2(dba)_3{\cdot}CHCl_3$. There have been several X-ray crystal structure determinations of $Pd^0_2(dba)_3{\cdot}$solvent (solvent = CH_2Cl_2[25] and $CHCl_3$;[34] for the former two ligands were found to be *s-cis,s-trans* and one ligand *s-cis,s-cis*, whereas the latter showed all ligands to be *s-cis,s-trans*).[26] The 'best structure' was reported by Pregosin and co-workers[27] in the late 1990s, which indicated that two of the dba ligands were disordered over two positions (around the 1,4-dien-3-one moieties),[28] that is complicated by conformational changes in the dba ligand (vis-à-vis *s-cis* and *s-trans* geometrical issues). Following many attempts over the last 10 years we are pleased to have accomplished a high-quality X-ray structure determination of $Pd^0_2(dba)_3{\cdot}CHCl_3$ (the crystallized $Pd^0_2(dba)_3{\cdot}CHCl_3$ was dissolved in fresh $CHCl_3$ and layered with hexane affording small purple crystals), giving final R indexes [$I \geq 2\sigma\ (I)$] R_1 = 0.0333, wR_2 = 0.0720 (monoclinic, $P2_1/n$ space group, Z = 4). The data show that all three ligands are disordered over two positions each, with a ratio of 79:21

dx.doi.org/10.1021/ja403259c | J. Am. Chem. Soc. 2013, 135, 8388–8399

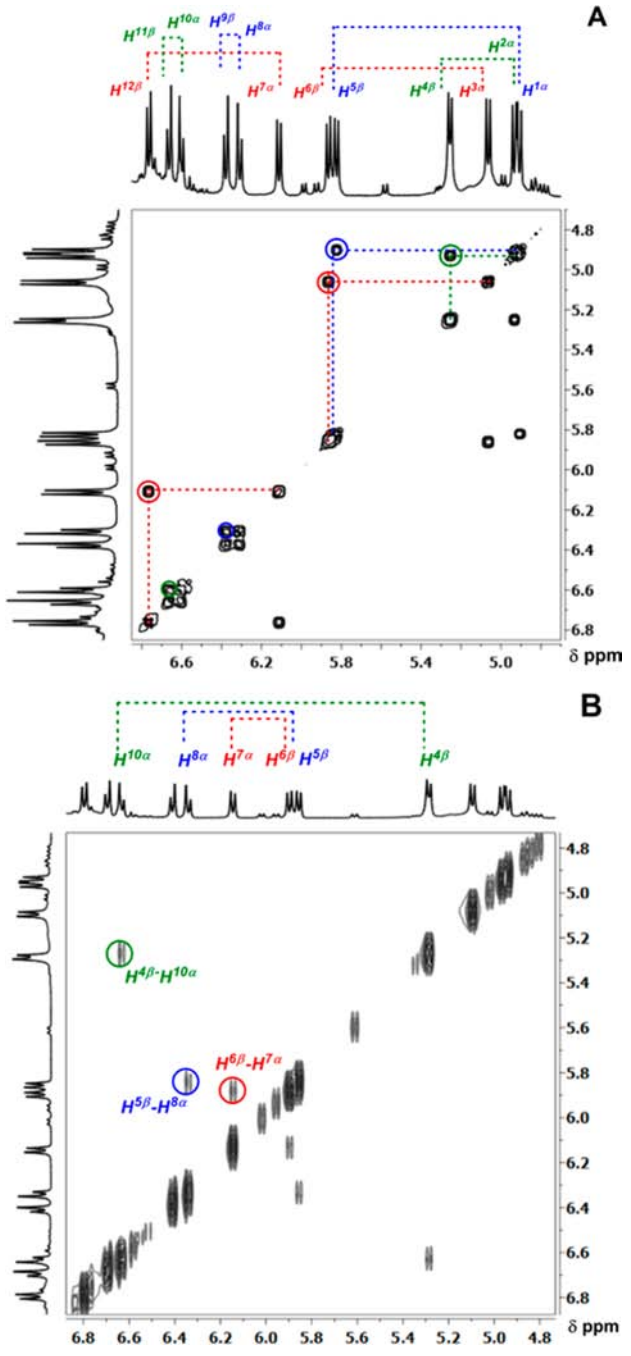

Figure 6. 700 MHz spectra of $Pd^0_2(dba)_3$ ($CDCl_3$, 238 K). (A) ^1H–COSY; (B) ^1H NOESY spectrum (correlations for major isomer).

(Figure 10; note the *s-cis* olefins are shown bonded in green and *s-trans* olefins shown bonded in orange). Both isomeric forms are shown for clarity (A and B). The Pd(1)–Pd(2) bond distance is 3.244 Å. The average *s-cis* C=C bond distances in isomer 1 is 1.3603 Å. For the *s-trans* C=C bonds the average distance is 1.393 Å. It is noticeable from the C–Pd bond distances that the *s-cis* C=C bonds are coordinating in an asymmetric fashion (average Cα–Pd = 2.247 Å, Cβ–Pd = 2.287 Å), whereas the *s-trans* C=C bonds are more symmetric (average Cα–Pd = 2.228 Å, Cβ–Pd = 2.229 Å), indicating that there is more back-bonding in the *s-trans* C=C bonds.[29]

Synthesis and Characterization of Pd^0_2(dba-Z)$_3$ Complexes. The Pd_2(dba-Z)$_3$·L complexes containing different

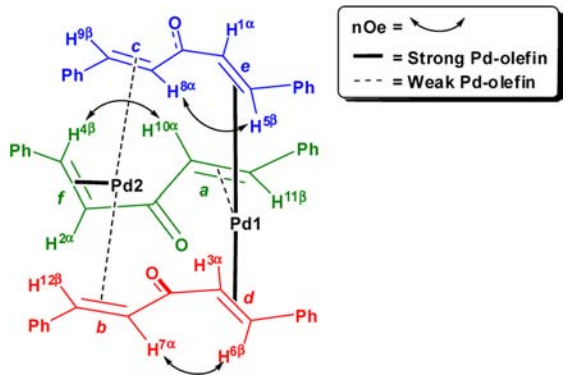

Figure 7. Proton connectivity in the major isomer of $Pd^0_2(dba)_3$, established by COSY and NOESY experiments.

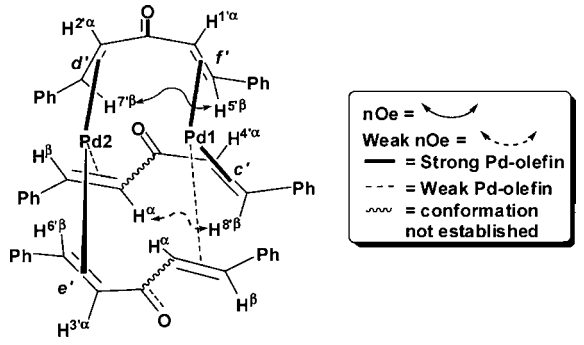

Figure 8. Proton connectivity in the minor isomer of $Pd^0_2(dba)_3$, established by COSY and NOESY experiments. Note that it was not possible to accurately assign the positions of 4 protons, which have not been numbered, but they are weakly coordinated.

Table 2. Relative Energies for $Pd^0_2(dba)_3$ Isomers by DFT

isomer	ΔE/kJmol^{-1}	$\Delta G_{298.15}$/kJmol^{-1}
Pd2(*s-Z*,*s-Z*,*s*-E), Pd1(*s-E*,*s-E*,*s-Z*), **M**	0	0
Pd2(*s-E*,*s-E*,*s-Z*), Pd1(*s-E*,*s-E*,*s-Z*), **N**	3	5
Pd2(*s-Z*,*s-E*,*s-Z*), Pd1(*s-Z*,*s-Z*,*s-E*), **O**	16	16
Pd2(*s-Z*,*s-Z*,*s-Z*), Pd1(*s-E*,*s-E*,*s-E*), **P**	26	23

dba-Z ligands with varying aryl substituents were prepared by the method described by Ishii in 1970 (procedure A, Figure 11).[30] A large stock solution of Na_2PdCl_4 in MeOH was used for the synthesis of several Pd_x(dba-Z)$_{x+1}$ complexes. The required dba-Z ligand (3 equiv) was added to a MeOH solution of Na_2PdCl_4 and heated to 60 °C until complete dissolution. The exact composition of this mixture remains unknown. A Pd^{II} complex, e.g., Na_nPdCl_{n+2}(dba-Z)$_2$, is a likely structure for the intermediate species, which is subsequently reduced. Six equiv of NaOAc were added to this solution, assisting the reduction process in alcoholic solvent ($Pd^{II} \rightarrow Pd^0$). On cooling solutions to ambient temperature the complexes precipitate as brown-maroon or purple solids (note: Pd black is formed in all cases—usually deposited on the glassware surface). Following precipitation from solution, which usually occurs at 60 °C, the complexes are filtered (at ambient temperature), washed with MeOH and water, and then dried *in vacuo* (on a glass frit); small quantities of acetone or acetone/water (1:2, *v*/*v*) can be used to improve the purity of the complexes (note: for the majority of the complexes some product dissolution was observed using acetone alone, which lowers the overall yields). A series of Pd_2(dba-Z)$_3$·L complexes were prepared in this

dx.doi.org/10.1021/ja403259c | J. Am. Chem. Soc. 2013, 135, 8388–8399

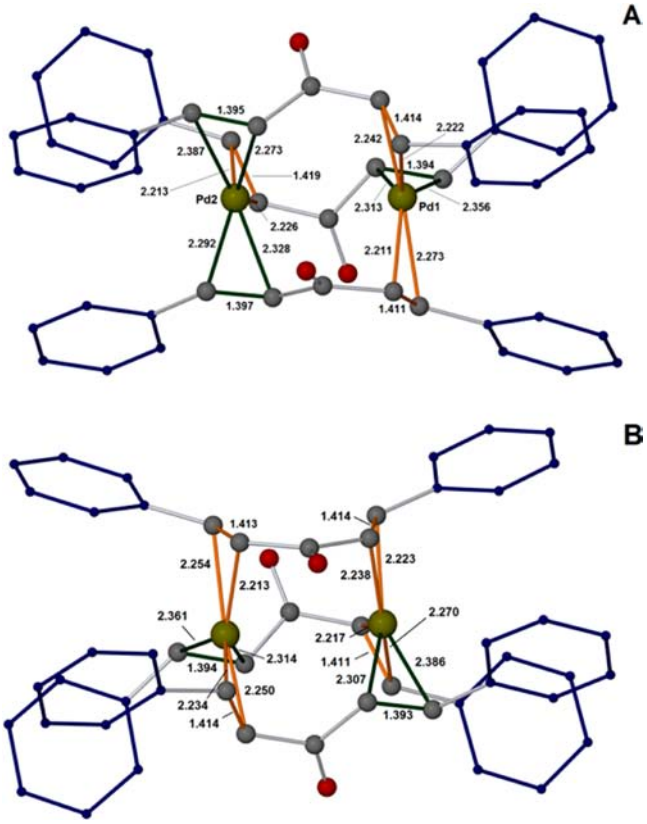

Figure 9. DFT calculated structures of (A) the major isomer of $Pd^0_2(dba)_3$ (**M**) and (B) the minor isomer of $Pd^0_2(dba)_3$ (**N**) (most likely isomers in solution). The bonds shown in green highlight the *s-cis* olefins and those shown in orange the *s-trans* olefins.

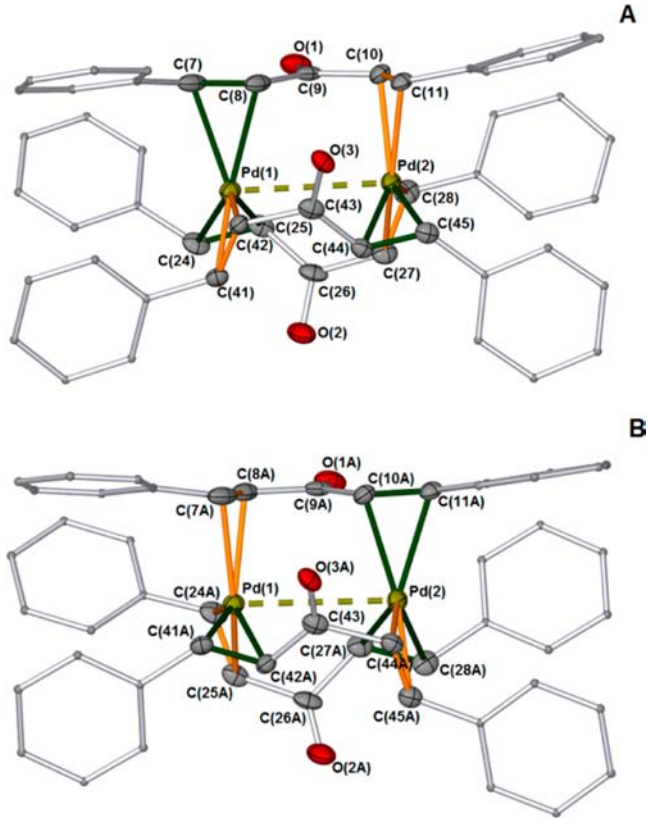

Figure 10. X-ray structure of $Pd^0_2(dba)_3{\cdot}CHCl_3$: (A) isomer 1; (B) isomer 2. Thermal ellipsoids set to 50% (not shown for the phenyl groups for reasons of clarity; H-atoms not shown). The fragmented bond denotes the Pd(1)···Pd(2) bond. The bonds shown in green highlight the *s-cis* olefins and those shown in orange the *s-trans* olefins (arbitrary atom numbering used).

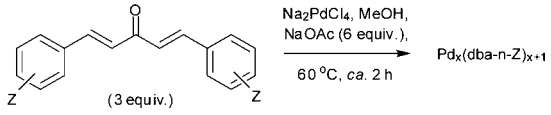

Figure 11. Synthesis of symmetrical $Pd_2(dba\text{-}Z)_3$.L complexes.

manner in acceptable yields (Table 3). The purity of the complexes was ascertained principally by element analysis (based on carbon and hydrogen percentage compositions). While one can ascertain the Pd:dba ratio for $Pd_2dba_3{\cdot}dba$ in $CDCl_3$ by ^1H NMR spectroscopy, we believe it is not suitable for assaying the purity of $Pd_2(dba\text{-}Z)_3{\cdot}L$ complexes, as they degrade to give Pd nanoparticles/particles in $CDCl_3$ (i.e., the outcome is dependent on the time between dissolution and spectroscopic analysis). This degradation process is well-known for $Pd^0_2(dba)_3$ in certain solvents[31] or reducing conditions, being a valuable precursor to Pd nanoparticles.[32]

For reactions where the dba-Z ligand was not fully dissolved, Pd^0 particle formation occurred quite readily (inferred by elemental analysis and low carbon and hydrogen composition and the appearance of fine particulate Pd black).[33]

It is pertinent to mention that several of these $Pd_2(dba\text{-}Z)_3{\cdot}L$ complexes react cleanly with PPh_3 (in DMF) to afford $Pd^0(\eta^2\text{-}dba\text{-}Z)(PPh_3)_2$ complexes, which have been characterized by NMR spectroscopic analysis and cyclic voltammetric methods.[11b]

We have also tested the synthesis of the $Pd_2(dba\text{-}Z)_3{\cdot}L$ complexes by the method described by Ishii in 1974 (procedure B),[34,35] from $PdCl_2$ [dba-Z ligand (3.3 equiv) and NaOAc (ca. 8 equiv) in MeOH, heated for 5 min at 50 °C, then $PdCl_2$ (1 equiv) added with heating for 4 h]. The $Pd_2(dba\text{-}4,4'\text{−}OHexyl)_3{\cdot}dba\text{-}4,4'\text{−}OHexyl$ complex was prepared by this procedure. Dissolution in $CHCl_3$ showed that '$Pd_2(dba\text{-}4,4'\text{−}OHexyl)_3$' was as stable as the parent complex (TEM analysis showed negligible Pd nanoparticle formation). $Pd_2(dba\text{-}4\text{-}t\text{-}Bu)_3{\cdot}dba\text{-}4\text{-}t\text{-}Bu$ was also synthesized via procedure B in a similar yield (78%).

Table 3. Yields of $Pd_2(dba\text{-}Z)_3{\cdot}L$ Complexes

$Pd_2(dba\text{-}Z)_3{\cdot}L$ (L = dba-Z or H_2O)	yield/%
$Pd_2(dba\text{-}3,4,5\text{-}OMe)_3$	59
$Pd_2(dba\text{-}3,5\text{-}OMe)_3{\cdot}dba\text{-}3,5\text{-}OMe$	53
$Pd_2(dba\text{-}4\text{-}OMe)_3$	72
$Pd_2(dba\text{-}4\text{-}OHexyl)_3{\cdot}dba\text{-}4\text{-}OHexyl$	70
$Pd_2(dba\text{-}4\text{-}t\text{-}Bu)_3$	75
$Pd_2(dba\text{-}4\text{-}F)_3{\cdot}H_2O$	80
$Pd_2(dba\text{-}4\text{-}CF_3)_3{\cdot}dba\text{-}4\text{-}CF_3$	69

^1H NMR Spectroscopic Analysis of $Pd_2(dba\text{-}Z)_3$ Complexes. ^1H NMR spectra of the $Pd_2(dba\text{-}Z)_3$ complexes in $CDCl_3$ (ca. 5 mg in 0.7 mL) were obtained (Figure 12). Complexes where Z = OMe possess limited solubility in $CDCl_3$ (especially 3,4,5-OMe and 3,5-OMe derivatives, spectra A and B, Figure 12). Moreover, within hours these complexes degrade in $CDCl_3$ (liberating free dba-Z ligand). Nevertheless a ^1H NMR spectral overlay shows that all the complexes exhibit diagnostic Pd^0-olefin interactions (ca. 5−7 ppm), akin to

dx.doi.org/10.1021/ja403259c | J. Am. Chem. Soc. 2013, 135, 8388−8399

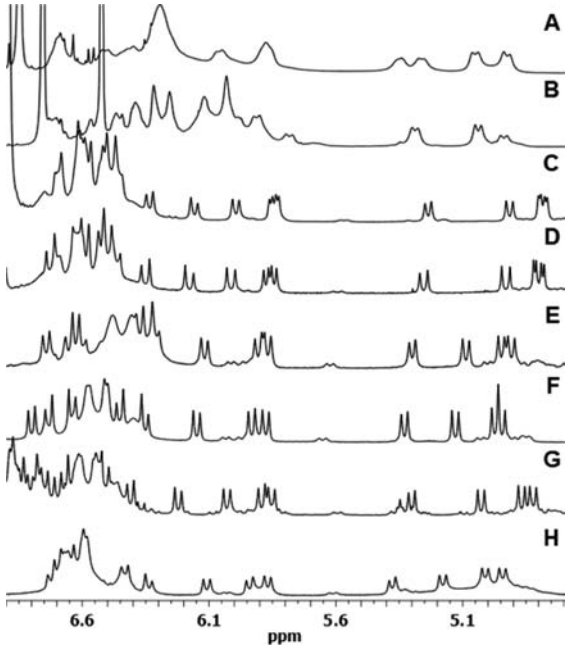

Figure 12. ^{1}H NMR spectra of $Pd^{0}_{2}(dba\text{-}Z)_3$ in $CDCl_3$ at 300 K (500 MHz, unless otherwise specified): (A) $Pd^{0}_{2}(dba\text{-}3,4,5\text{-}OMe)_3$; (B) $Pd^{0}_{2}(dba\text{-}3,5\text{-}OMe)_3$; (C) $Pd^{0}_{2}(dba\text{-}4\text{-}OMe)_3$; (D) $Pd^{0}_{2}(dba\text{-}4\text{-}OHexyl)_3$ (note 400 MHz spectrum); (E) $Pd^{0}_{2}(dba\text{-}4\text{-}t\text{-}Bu)_3$; (F) $Pd^{0}_{2}(dba)_3$; (G) $Pd^{0}_{2}(dba\text{-}4\text{-}F)_3$; (H) $Pd^{0}_{2}(dba\text{-}4\text{-}CF_3)_3$.

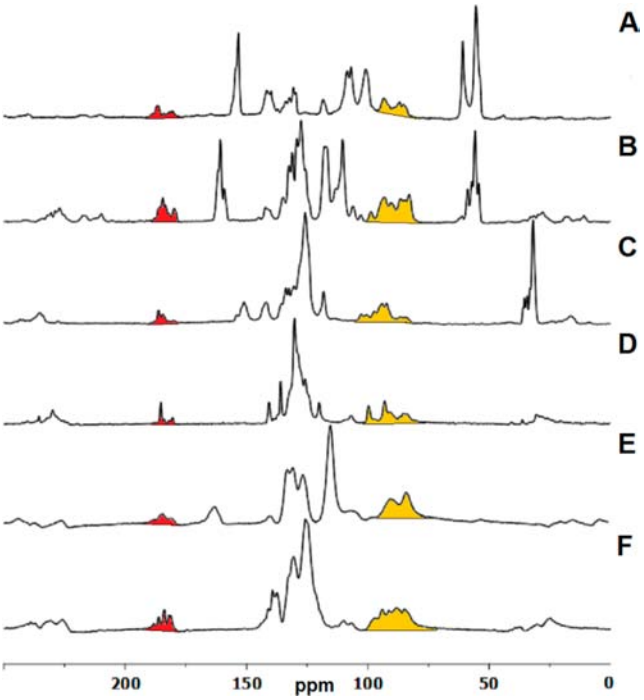

Figure 13. Selected ^{13}C-MAS spectra [100.56 MHz (recycle delays ca. 2−5 s, spin rate ca. 10 kHz)] of the $Pd_2(dba\text{-}Z)_3$ complexes: (A) $Pd^{0}_{2}(dba\text{-}3,4,5\text{-}OMe)_3$; (B) $Pd^{0}_{2}(dba\text{-}4\text{-}OMe)_3$; (C) $Pd^{0}_{2}(dba\text{-}4\text{-}t\text{-}Bu)_3$; (D) $Pd^{0}_{2}(dba)_3$; (E) $Pd^{0}_{2}(dba\text{-}4\text{-}F)_3$; (F) $Pd^{0}_{2}(dba\text{-}4\text{-}CF_3)_3$. Peaks colored orange are attributed as Pd-olefin carbon signals and red are attributed carbonyl signals.

$Pd^{0}_{2}(dba)_3$. That is in most cases there are 12 olefinic protons as expected in these dinuclear Pd complexes. ^{1}H COSY spectra of several complexes exhibit proton−proton correlations that are similar to $Pd^{0}_{2}(dba)_3$. We did not observe spectral broadening for $Pd_2(dba\text{-}4\text{-}OMe)_3$ and $Pd_2(dba\text{-}4\text{-}OHexyl)_3$.

Some broadening is observed for $Pd_2(dba\text{-}4\text{-}CF_3)_3$, although the signals for the major isomer are relatively sharp. Minor isomers for several of these complexes (uncharacterized) are evidenced by the small peaks in the ^{1}H NMR spectra, akin to $Pd_2(dba)_3$.

It is interesting to note that the position (chemical shift) of the olefin protons is affected to a certain degree by the remote aryl substituents, indicative of electronic communication in the complexes and in keeping with the electronic differences observed at the olefins in dba-Z derivatives.[12,36] Particularly noticeable is the shift of the most shielded olefin protons, H1 and H2, in spectra C and D in Figure 12.

The limited solubility of the $Pd^{0}_{2}(dba\text{-}Z)_3$ complexes prevented their solution ^{13}C NMR spectra from being obtained. However, the solid-state ^{13}C MAS spectra of a number of complexes gave some useful information (Figure 13). The parent complex, $Pd^{0}_{2}(dba)_3$, exhibits ^{13}C signals for Pd-olefins (ca. δ 80−105 ppm) and carbonyl moieties (ca. δ 180 ppm). Spinning side-bands are observed on the outer edges of the spectrum. For $Pd^{0}_{2}(dba\text{-}4\text{-}F)_3$ the intrinsic line width is quite high (spectral resolution is relatively limited), which could be a result of fluorine being in the system. For all other complexes there is a hint that the intrinsic line widths are relatively low, i.e., there are a high number of overlapping lines with similar shifts that limits the resolution, evidence for ligand inequivalence in each complex and multiple structures (i.e., conformers) in the asymmetric unit. It is important to emphasize that the solid-state structures of the $Pd^{0}_{2}(dba\text{-}Z)_3$ complexes mirror that of $Pd^{0}_{2}(dba)_3$ by ^{13}C MAS NMR.

X-ray Structures of Selected $Pd_2(dba\text{-}Z)_3$·L Complexes. Three $Pd_2(dba\text{-}Z)_3$ complexes (Z = 3,5-OMe, 4-OMe, and 4-F) could be crystallized from a CH_2Cl_2 solution layered with diethyl ether at room temperature. As with $Pd_2(dba)_3$·$CHCl_3$ we were able to obtain X-ray diffraction data for which structural refinement was possible. For example $Pd_2(dba\text{-}3,5\text{-}OMe)_3$·$CH_2Cl_2$ crystallized in the $P2_1/c$ space group (monoclinic, Z = 4) (Figure 14). The two alkenes in each ligand coordinating both Pd^0 centers are essentially eclipsed. Interestingly, the complex contains one dba-3,5-OMe ligand that can be found over two positions (occupancy = 0.682(3):0.318(3) or ca. 2.1:1). Similar disorder was noted for $Pd_2(dba\text{-}H)_3$·CH_2Cl_2 *vide supra*. The phenyl moieties and positions of the carbonyl groups in both conformers were resolved in the case of $Pd_2(dba\text{-}3,5\text{-}OMe)_3$·$CH_2Cl_2$. In essence, for each conformer there is a strict requirement for these moieties to exhibit different orientations. The Pd···Pd distance is 3.2314(5) Å, which compares with 3.244 Å in our X-ray structure of $Pd_2(dba\text{-}H)_3$·$CHCl_3$ and is indicative of a nonbonding interaction; the electron count on each Pd^0 center is 16. The tightly packed structure of $Pd_2(dba\text{-}3,5\text{-}OMe)_3$·$CH_2Cl_2$ is also illustrated in Figure 14, which shows that each Pd^0 atom is effectively shielded from solvent (or other ligands) in the solid state. There is also significant steric congestion between the 3,5-methoxy substituents in neighboring dba-3,5-OMe ligands.

Considering the major isomer of [$Pd_2(dba\text{-}3,5\text{-}OMe)_3$·$CH_2Cl_2$], it is instructive to compare the C═C bond lengths of the coordinated ligand to each Pd center (Figure 15). For Pd1 the C═C bond, C(52A)−C(53A), orientated *s-trans* to the C═O group is significantly longer than the other two C═C bonds, one orientated *s-cis*, C(10)−C(11), and the other

dx.doi.org/10.1021/ja403259c | J. Am. Chem. Soc. 2013, 135, 8388−8399

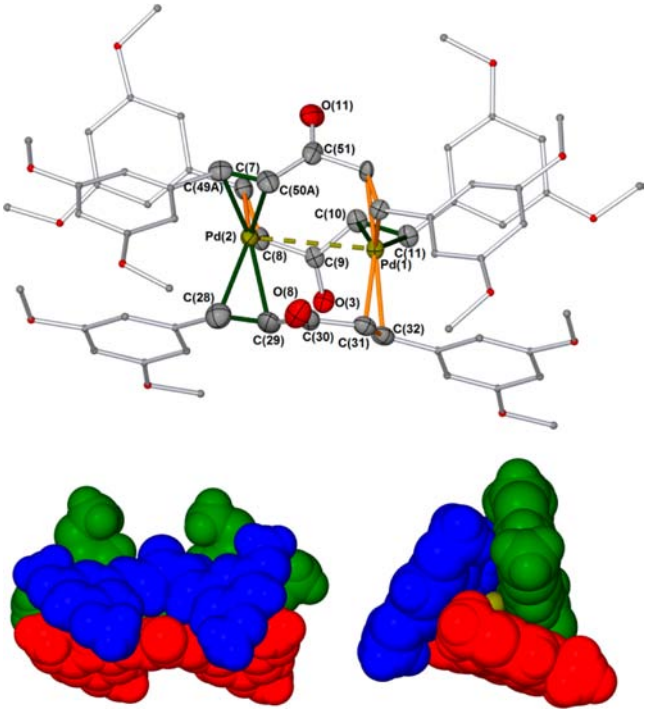

Figure 14. Top: X-ray structure of Pd_2(dba-3,5-OMe)$_3$·CH_2Cl_2. Hydrogens and 1 CH_2Cl_2 molecule omitted for clarity; one dba-3,5-OMe ligand is found over 2 positions [i.e., C(49A)-C(50A) and C(52A)-C(53A)] (only one ligand position shown). The bonds shown in green highlight the *s-cis* olefins and those shown in orange the *s-trans* olefins (arbitrary atom numbering used). Bottom: Space-filling models (each ligand has been colored red, blue and green to allow differentiation), left - side-on perspective and right - end-on perspective.

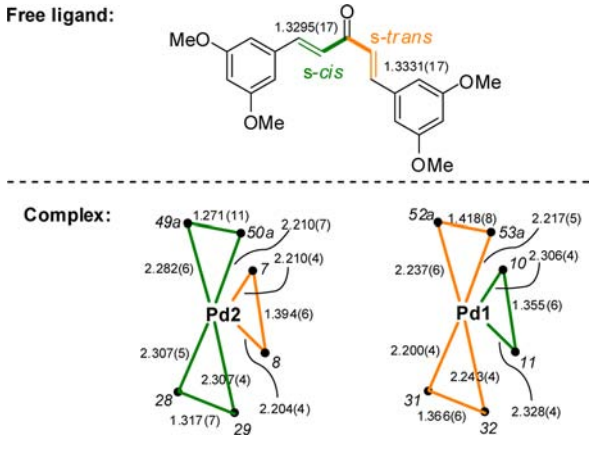

Figure 15. Selected bond lengths (X-ray diffraction data) of the olefins in the free ligand, dba-3,5-OMe, and Pd_2(dba-3,5-OMe)$_3$·CH_2Cl_2. We note that C49a−C50a is a particularly short C═C bond (larger estimated standard deviations are observed within the disordered ligand). The bonds shown in green highlight the *s-cis* olefins and those shown in orange the *s-trans* olefins.

s-trans, C(31)−C(32). The latter *s-cis* and *s-trans* C═C bonds are identical (within the error limits).

For Pd2 it is apparent that the C═C bond orientated *s-trans* to the C═O group, C(7)−C(8), is significantly longer than the two C═C bonds orientated *s-cis*, C(28)−C(29) and C(49A)-C(50A) (for the latter, foreshortening of this C═C bond can be explained in part by excessive thermal motion). Thus, for each palladium center there is a *s-trans* C═C bond that is substantially longer than the other C═C bonds, indicative of back-bonding. The free ligand dba-3,5-OMe (see SI for X-ray structure) was found to (fortuitously) adopt a *s-cis,s-trans* conformation in a single crystal, with both C═C bonds showing the same distance (within error). The longest C═C bond, C(52A)−C(53A) in the complex is ca. 0.09 Å longer than the same bond in the free ligand.

The X-ray diffraction data for Pd_2(dba-4-OMe)$_3$·CH_2Cl_2 (monoclinic, $P2_1/n$ space group, Z = 4) and Pd_2(dba-4-F)$_3$·CH_2Cl_2 (triclinic, $P\bar{1}$, Z = 2) show that dba-Z ligand disorder is seen about the 1,4-dien-3-one moieties. In the case of Pd_2(dba-4-F)$_3$·CH_2Cl_2 each dba-4-F ligand is disordered over two positions; all could be satisfactorily modeled in a similar manner to Pd^0_2(dba)$_3$·$CHCl_3$ (*vide supra*). The solvate molecules of crystallization appear to be crucial. In this context the X-ray structure[37] of Pd^0_2(dba-4,4′−OH)$_3$ requires further examination. In this structure extensive H-bonding interactions between neighboring hydroxyls and carbonyl groups lock and stabilize the structure (Figure 16), which leads to only one isomeric form being observed in the solid-state. This is a unique case and stands in contrast to the other related structures detailed in this paper.

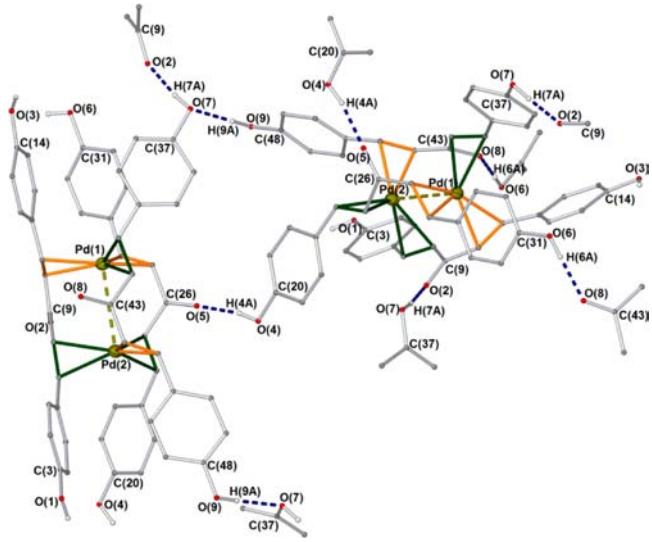

Figure 16. H-bonding network seen for Pd^0_2(dba-4,4′-OH)$_3$. Key H-bonding interactions (shown as blue fragmented bonds): O(2)···H-(7A)−O(7) = 1.689 Å, O(5)···H(4A)−O(4) = 1.819 Å, O(7)···H-(9A)−O(9) = 1.910 Å, O(8)···H(6A)−O(6) = 1.806 Å. The bonds shown in green highlight the *s-cis* olefins and those shown in orange the *s-trans* olefins.

■ CONCLUSION

The solution and solid-state structures of Pd^0_2(dba)$_3$ and Pd^0_2(dba-Z)$_3$-type complexes have been comprehensively determined. In the case of the former parent complex isotopic labeling (^{2}H and ^{13}C) was necessary to determine the solution structures of the freely exchanging major and minor isomers of Pd^0_2(dba)$_3$; in the case of the major isomer of Pd^0_2(dba)$_3$ this is unambiguous. It consists of three *s-cis,s-trans* ligands, where the *s-cis* olefins are weakly bound to Pd^0 and the *s-trans* olefins strongly bound. Asymmetric dba coordination results, with one Pd^0 atom coordinated to two *s-trans* olefins and one *s-cis* olefin, and the second Pd^0 atom coordinated to two *s-cis* olefins and

dx.doi.org/10.1021/ja403259c | J. Am. Chem. Soc. 2013, 135, 8388−8399

one *s-trans* olefin. The minor isomer of $Pd^0_2(dba)_3$ possesses a *s-trans,s-trans* ligand and the chemical shifts of the *β*-protons indicate that four of the six olefins are *s-trans* and strongly bound to both Pd^0 centers, with other two olefins being *s-cis*. This study brings about a resolution to the confounding molecular structure[18,22] of this ubiquitous complex in solution.

Theoretical calculations (DFT) support the feasibility of the experimentally determined major and minor isomeric structures in solution. The major isomer of $Pd^0_2(dba)_3$ contained three bridging dba ligands found exclusively in a *s-cis,s-trans* conformation. The minor isomer of $Pd^0_2(dba)_3$ reveals that one dba ligand is found exclusively in a *s-trans,s-trans* conformation. A high-resolution X-ray structure determination of $Pd^0_2(dba)_3{\cdot}CHCl_3$ shows that all three dba ligands are disordered over two positions, which is an issue associated with the conformational flexibility around the 1,4-dien-3-one moiety in the solid-state.

NMR spectroscopic analysis of $Pd^0_2(dba\text{-}Z)_3$ reveals that the aryl substituent has a profound effect on the rate of Pd-olefin exchange (evidenced by the relative sharpness of their ^1H NMR spectra), in addition to their stability in solution (e.g., in $CDCl_3$). The solid-state structures of three $Pd^0_2(dba\text{-}Z)_3{\cdot}$solvent complexes (4-F, 4-OMe, 3,5-OMe) have been determined by single crystal X-ray diffraction methods. As with $Pd^0_2(dba)_3{\cdot}CHCl_3$, varying degrees of dba-Z disorder were observed, where the Z-substituent affects the distribution of isomers produced, an observation especially noticeable in the solid-state.

EXPERIMENTAL SECTION

General details for this section (NMR, MS, IR, UV–vis, X-ray, elemental analysis, TEM) are detailed in the SI. Important synthetic procedures and characterization data are presented below. Deuterium-labeled $Pd^0_2(D(2,4)\text{-dba-}PhD_5)_3{\cdot}D(2,4)\text{-dba-}PhD_5$, $Pd^0_2(D(1,5)\text{-dba-}PhD_5)_3{\cdot}D(1,5)\text{-dba-}PhD_5$, and $Pd^0_2(dba\text{-}PhD_5)_3{\cdot}dba\text{-}PhD_5$ complexes have been previously reported.[18] Details of the ^{13}C-labeled dba compounds, and all other dba-Z ligands, are given in the SI (including representative NMR spectra).

General Synthesis of $Pd_2(dba)_3{\cdot}L$ and $Pd_2(dba\text{-}Z)_3{\cdot}L$ (L = dba/dba-Z or solvate). Procedure A: NaCl (3.28 g, 56 mmol) was added to a solution of $PdCl_2$ (4.97 g, 28 mmol) in methanol (140 mL) and stirred at ambient temperature under an inert atmosphere for 24 h. The dark-brown solution was then filtered through a plug of cotton wool and concentrated *in vacuo* to approximately one-half of its original volume. The solution was warmed to 60 °C, and then dba (88 mmol, 3.1 equiv) was added (or dba-Z). The resulting mixture was stirred at 60 °C for 15 min, and then sodium acetate (13.78 g, 0.168 mol, 6 equiv) was added. The mixture was allowed to cool to ambient temperature (with no external cooling) and stirred for 2 h until a dark-red/purple precipitate was observed, which was filtered and washed with methanol (2 × 100 mL), water (2 × 50 mL), and finally acetone (2 × 5 mL). The product was partially dried under suction. The solid was transferred to a Schlenk flask and slowly dried by passage of nitrogen gas (with stirring) overnight. This gave the desired complexes as maroon/purple microcrystalline solids. These reactions work on a scale as low as ca. 0.1 g $PdCl_2$, in addition to using aliquots from stock solutions of Na_2PdCl_4 in methanol.

Procedure B: This procedure is similar to that reported by Ishii and co-workers[34] ($PdCl_2$, dba or dba-Z, NaOAc in MeOH at 40–50 °C) and by our group[16] for $Pd^0_2(th_n\text{-dba})_3{\cdot}th_n\text{-dba}$ derivatives.

Characterization data for $Pd_2(dba)_3{\cdot}CHCl_3$: Anal. calcd for $C_{52}H_{43}O_3Pd_2Cl_3$ (1135.09), C 60.34, H 4.19; Found, C 60.25, H 4.3. Single crystals of this pure material were grown from a saturated $CHCl_3$ solution layered with hexane, which gave purple rod-like crystals, from which one single crystal was selected for X-ray diffraction. Also noted were the formation of hexagon crystals, however the X-ray diffraction data quality was poor, and a reasonable structure could not be determined.

Characterization Data for $Pd_2(dba\text{-}Z)_3{\cdot}dba\text{-}Z$. In all cases the minor isomer could not be fully assigned, therefore the proton signals given are for the major isomer. The aromatic regions are broad in all cases; overlapping signals are observed for both major and minor isomeric forms for each complex. In all cases where resolved olefin proton signals are observed, we propose that the ligands adopt a *s-cis,s-trans* conformation, i.e., having a similar structure to the major isomer of $Pd^0_2(dba)_3$. The reactions were typically run using 0.1–0.25 g of $PdCl_2$.

$[Pd^0_2(dba\text{-}4\text{-}F)_3{\cdot}H_2O]$. Yield = 80%; Mp 134–136 °C; UV (THF, nm) 518 (d–d); ^1H NMR 4.82 (1H, d, $^3J_{HH}$ = 12.5 Hz, H1), 4.87 (1H, d, $^3J_{HH}$ = 12.5 Hz, H2), 5.03 (1H, d, $^3J_{HH}$ = 13 Hz, H3), 5.30 (1H, d, $^3J_{HH}$ = 12.5 Hz, H4), 5.85 (1H, d, $^3J_{HH}$ = 13.5 Hz, H5), 5.89 (1H, d, $^3J_{HH}$ = 13 Hz, H6), 6.03 (1H, d, $^3J_{HH}$ = 13.5 Hz, H7), 6.22 (1H, d, $^3J_{HH}$ = 13 Hz, H8), 6.41 (1H, d, $^3J_{HH}$ = 13.5 Hz, H9), 6.44–7.03 (ca. 27 H, ArH, 3 olefin protons H10–H12); Anal. calcd for $C_{51}H_{38}F_6O_4Pd_2$ (1041.68), C 58.80, H 3.68; Found, C 58.95, H 4.10. Crystals suitable for X-ray analysis were grown from a CH_2Cl_2 solution of the complex (ca. 20 mg) layered with diethyl ether.

$[Pd^0_2(dba\text{-}4\text{-}t\text{-}Bu)_3]$. Yield = 75%; Mp 139–140 °C; UV (THF, nm) 533 (d-d); ^1H NMR 4.91 (1H, d, $^3J_{HH}$ = 13 Hz, H1), 4.95 (1H, d, $^3J_{HH}$ = 12.5 Hz, H2), 5.09 (1H, d, $^3J_{HH}$ = 13 Hz, H3), 5.30 (1H, d, $^3J_{HH}$ = 12 Hz, H4), 5.87 (1H, d, $^3J_{HH}$ = 13.5 Hz, H5), 5.91 (1H, d, $^3J_{HH}$ = 13 Hz, H6), 6.12 (1H, d, $^3J_{HH}$ = 13 Hz, H7), 6.31 (1H, d, $^3J_{HH}$ = 13.5 Hz, H8), 6.37 (1H, d, $^3J_{HH}$ = 13.5 Hz, H9), 6.60 (1H, d, $^3J_{HH}$ = 13.5 Hz, H10), 6.65 (1H, d, $^3J_{HH}$ = 13.5 Hz, H11), 6.74 (1H, d, $^3J_{HH}$ = 13.5 Hz, H12), 6.39–6.54 (ca. 6H, br m, overlapping with olefin protons H9–H10), 6.93–7.21 (ca. 12H, br m). Note: *t*-Bu protons overlapping with free ligand at *δ* 1.34; ESI-MS: *m/z* 821.1 $[Pd(dba\text{-}4\text{-}t\text{-}Bu)_2 + Na]^+$ (6), 929.1 $[Pd_2(dba\text{-}4\text{-}t\text{-}Bu)_2Na]^+$ (58); Anal. calcd for $C_{75}H_{90}O_3Pd_2$ (1252.36), C 71.93, H 7.24; Found, C 72.31, H 6.77. Crystals were grown from a CH_2Cl_2 solution of the complex (ca. 20 mg) layered with diethyl ether, however these gave poor quality X-ray diffraction data (a cif file is available from the authors).

$[Pd^0_2(dba\text{-}4\text{-}OMe)_3]$. Yield = 72%; Mp 141–143 °C; UV (THF, nm) 533 (d–d); ^1H NMR 4.78 (1H, d, $^3J_{HH}$ = 12.5 Hz, H1), 4.79 (1H, d, $^3J_{HH}$ = 12 Hz, H2), 4.91 (1H, d, $^3J_{HH}$ = 13 Hz, H3), 5.24 (1H, d, $^3J_{HH}$ = 12 Hz, H4), 5.84 (1H, d, $^3J_{HH}$ = 12.5 Hz, H5), 5.85 (1H, d, $^3J_{HH}$ = 12.5 Hz, H6), 5.99 (1H, d, $^3J_{HH}$ = 13 Hz, H7), 6.16 (1H, d, $^3J_{HH}$ = 13 Hz, H8), 6.33 (1H, d, $^3J_{HH}$ = 13 Hz, H9), ca. 6.1–7.5 (ca. 27H, br m, overlapping with olefin protons H10–H12). Note: Overlapping methoxy signals at *δ* 3.79, 3.80, and 3.82 (broad signals); ESI-MS: *m/z* (%) = 716.9 $[Pd(dba\text{-}4\text{-}OMe)_2 + Na]^+$ (6), 824.9 $[Pd_2(dba\text{-}4\text{-}OMe)_2Na]^+$ (66), 929.9 $[Pd_3(dba\text{-}4\text{-}OMe)_2Na]^+$ (61), 1035.8 $[Pd_4(dba\text{-}4\text{-}OMe)_2Na]^+$ (84); Anal. calcd for $C_{57}H_{54}O_9Pd_2$ (1095.87), C 62.47, H 4.97; Found, C 62.03, H 4.95. Crystals suitable for X-ray analysis were grown from a CH_2Cl_2 solution of the complex (ca. 20 mg) layered with diethyl ether.

$[Pd^0_2(dba\text{-}4\text{-}OHexyl)_3{\cdot}dba\text{-}4\text{-}OHexyl]$. Yield = 70%; Mp 104–107 °C; UV ($CDCl_3$, nm) 540 (d–d); ^1H NMR 4.79 (1H, d, $^3J_{HH}$ = 12.5 Hz, H1), 4.80 (1H, d, $^3J_{HH}$ = 12 Hz, H2), 4.93 (1H, d, $^3J_{HH}$ = 13 Hz, H3), 5.25 (1H, d, $^3J_{HH}$ = 12 Hz, H4), 5.85 (1H, d, $^3J_{HH}$ = 12.5 Hz, H5), 5.87 (1H, d, $^3J_{HH}$ = 13 Hz, H6), 6.01 (1H, d, $^3J_{HH}$ = 13 Hz, H7), 6.18 (1H, d, $^3J_{HH}$ = 13.5 Hz, H8), 6.35 (1H, d, $^3J_{HH}$ = 13.5 Hz, H9), 6.41–6.80 (ca. 27H, br m, overlapping with olefin protons H10–H12). Note: Overlapping alkyl protons with free ligand at 0.92, 1.35, 1.48, 1.80, and 3.98 (broad signals). LIFDI-MS: *m/z* (%) = 1516.9 $[Pd_2(dba\text{-}4\text{-}OHexyl)_3]^{\bullet+}$ (100); 1516.66 (calcd); Anal. calcd for $C_{116}H_{152}O_{12}Pd_2$ (1515.66), C 71.4, H 7.85; Found, C 71.61, H 7.76.

$[Pd^0_2(dba\text{-}4\text{-}CF_3)_3{\cdot}dba\text{-}4\text{-}CF_3{\cdot}H_2O]$. Yield = 69%; Mp 151–152 °C; UV (THF, nm) 534 (d–d); ^1H NMR 4.95 (1H, d, $^3J_{HH}$ = 13 Hz, H1), 5.02 (1H, d, $^3J_{HH}$ = 12.5 Hz, H2), 5.19 (1H, d, $^3J_{HH}$ = 13 Hz, H3), 5.39 (1H, d, $^3J_{HH}$ = 12.5 Hz, H4), 5.88 (1H, d, $^3J_{HH}$ = 13 Hz, H5), 5.95 (1H, d, $^3J_{HH}$ = 13 Hz, H6), 6.12 (1H, d, $^3J_{HH}$ = 13 Hz, H7), 6.35 (1H, d, $^3J_{HH}$ = 13.5 Hz, H8), 6.45 (1H, d, $^3J_{HH}$ = 13.5 Hz, H9), 6.41–6.80 (ca. 15H, br m, overlapping with olefin protons H10–H12), 7.27–7.58 (ca. 12H, br m); ESI-MS: *m/z* (%) = 846 $[Pd_1(dba\text{-}4\text{-}$

dx.doi.org/10.1021/ja403259c | J. Am. Chem. Soc. 2013, 135, 8388–8399

$CF_3)_2]^+$ (10), 975 $[Pd_2(dba\text{-}4\text{-}CF_3)_2Na]^+$ (15); Anal. calcd for $C_{36}H_{26}F_{12}O_3Pd$ (865.01), C 52.76, H 3.03; Found, C 52.72, H 2.98.

[Pd^0_2(dba-3,5-OMe)$_3$·dba-3,5-OMe]. Due to the broadness of the proton signals the proton integrals are not reliable; selected data is therefore quoted (i.e., the peaks observed). The observed spin−spin coupling constants are averaged because of the exchange on the NMR time scale (due to intra- and intermolecular exchange). Yield = 53%; Mp 134−135 °C; UV (THF, nm) 530 (d−d); ^{1}H NMR 4.94 (1H, d, 12 Hz, H1), 5.04 (2H, d, 12 Hz, H2/H3), 5.29 (2H, d, 12 Hz, H4/H5), 5.78 (1H, d, 12 Hz, H6), ca. 6.2−7.5 (ca. 24 H, overlapping with olefin protons H7−H12). Note: Overlapping methoxy signals at δ 3.57−3.77 (broad signals). The free ligand exhibits a methoxy signal at 3.84; ESI-MS: m/z (%) = 838.9 $[Pd_1(dba\text{-}3,5\text{-}OMe)_2 + Na]^+$ (14), 944.9 $[Pd_2(dba\text{-}3,5\text{-}OMe)_2Na]^+$ (100); Anal. calcd for $C_{42}H_{44}O_{10}Pd$ (815.21), C 61.88, H 5.44; Found, C 62.55, H 5.19. Crystals suitable for X-ray analysis were grown from a CH_2Cl_2 solution of the complex (ca. 20 mg) layered with diethyl ether.

[Pd^0_2(dba-3,4,5-OMe)$_3$]. Due to the broadness of the proton signals, the proton integrals are not reliable; selected data is therefore quoted (i.e., the peaks observed). Yield = 59%; Mp 194−197 °C; UV (THF, nm) 529 (d−d); ^{1}H NMR 4.92 (2H, d, 11 Hz, H1/H2), 5.05 (2H, d, 11 Hz, H3/H4), 5.21−5.31 (broad signal), 5.30−5.42 (broad signal), 5.82−5.93 (broad signal), 6.02−6.10 (broad signal), 6.17−6.55 (broad signal), 6.65−6.76 (broad signal). Note: Overlapping methoxy signals at 3.62, 3.68, 3.80, and 3.83 (broad signals). The liberated ligand exhibits methoxy signals at 3.90 and 3.92; Anal. calcd for $C_{69}H_{78}O_{21}Pd_2$ (1456.19), C 56.91, H 5.40; Found, C 57.31, H 5.46.

Details of DFT Calculations. All calculations were performed using the TURBOMOLE V5.10 package using the resolution of identity (RI) approximation.[38] Initial optimizations were performed at the (RI-)BP86/SV(P) level, followed by frequency calculations at the same level. All minima were confirmed as such by the absence of imaginary frequencies. Energies, geometries, and vibrational frequencies are presented in the SI. Single-point calculations on the (RI-)BP86/SV(P) optimized geometries were performed using the hybrid PBE0 functional and the flexible def2-TZVPP basis set. The (RI-)PBE0/def2-TZVPP SCF energies were corrected for their zero point energies (ΔE), thermal energies, and entropies (obtained from the (RI-)BP86/SV(P)-level frequency calculations at 298.15 K, $\Delta G_{298.15}$). In all calculations, a 28 electron quasi-relativistic ECP replaced the core electrons of Pd. No symmetry constraints were applied during optimizations.

■ ASSOCIATED CONTENT

Supporting Information

All other synthetic procedures, characterization data (representative spectra), details, and X-ray diffraction details. This material is available free of charge via the Internet at http://pubs.acs.org.

■ AUTHOR INFORMATION

Corresponding Author

ian.fairlamb@york.ac.uk

Present Address

†Department of Chemistry, Institute of Chemical Technology, Matunga, Mumbai-400019, India

Notes

The authors declare no competing financial interest.

■ ACKNOWLEDGMENTS

We are grateful to Heather Fish, Prof. Simon Duckett, and Dr. Ryan Mewis for assistance with several NMR experiments. Ms. Qiong Xu and Mr. Josh Bray are thanked for their contributions to this project (particularly on the stability of $Pd^0_2(dba)_3$ and Pd^0_2(dba-4-Ohexyl)$_3$ complexes). Dr. Petr Sehnal is thanked for crystallizing dba-3,5-OMe. We thank Prof. Felix Goodson for providing the X-ray cif file for Pd^0_2(dba-4,4′-OH)$_3$. Prof. Cortlant Pierpont is thanked for sharing his X-ray diffraction data analysis on $Pd^0_2(dba)_3$. The Royal Society is thanked for funding a University Research Fellowship (I.J.S.F.). The research leading to these results has received funding from the Innovative Medicines Initiative Joint Undertaking under grant agreement no. 115360, resources of which are composed of financial contribution from the European Union's Seventh Framework Programme (FP7/2007-2013) and EFPIA companies' in kind contribution (PhD studentship for A.J.R.). We gratefully acknowledge use of the Esquire ESI-MS instrument in the York Centre of Excellence in Mass Spectrometry, which was created thanks to a major capital investment through Science City York, supported by Yorkshire Forward with funds from the Northern Way Initiative. We thank EPSRC for funding (PhD funding for T.J.W., grant code EP/P505178/1; Computational Cluster, grant code EP/H011455/1).

■ REFERENCES

(1) (a) Littke, A. F.; Fu, G. C. *Angew. Chem., Int. Ed.* **2002**, *41*, 4176−4211. (b) Nolan, S. P. In *N-Heterocyclic Carbenes in Synthesis*; Wiley-VCH: Weinheim, 2006, pp 1−304. (c) Glorius, F. N.Topics in Organometallic Chemistry. In *Heterocyclic Carbenes in Transition Metal Catalysis*; Springer-Verlag: Berlin, 2006, Vol. *21*, pp 1−218. (d) de Meijere, A.; Diederich, F. In *Metal Catalyzed Cross-Coupling Reactions*; Wiley-VCH: Weinheim, 2004, Vol. *II*.

(2) Moulton, B. E..; Duhme-Klair, A. -K.; Fairlamb, I. J. S.; Lynam, J. M.; Whitwood, A. C. *Organometallics* **2007**, *26*, 6354−6365.

(3) (a) Amatore, C.; Jutand, A. *Coord. Chem. Rev.* **1998**, *178−180*, 511−528. (b) Amatore, C.; Jutand, A.; Meyer, G. *Inorg. Chim. Acta* **1998**, *273*, 76−84. (c) Jarvis, A. G.; Fairlamb, I. J. S. *Curr. Org. Chem.* **2011**, *22*, 3175−3196.

(4) Fairlamb, I. J. S. In *Encyclopedia of Reagents for Organic Synthesis*, John Wiley & Sons, Ltd: Hoboken, NJ, 2008; DOI: 10.1002/047084289X.rt400.pub2.

(5) (a) Amatore, C.; Jutand, A.; Khalil, F.; M'Barki, M. A.; Mottier, L. *Organometallics* **1993**, *12*, 3168−3178. (b) Fairlamb, I. J. S. *Org. Biomol. Chem.* **2008**, *6*, 3645−3656.

(6) The π-acidic alkene can increase catalyst stability, see: (a) Scrivanti, A.; Beghetto, V.; Matteoli, U.; Antonaroli, S.; Marini, A.; Mandoj, F.; Paolesse, R.; Crociani, B. *Tetrahedron Lett.* **2004**, *45*, 5861−5864. (b) Scrivanti, A.; Beghetto, V.; Matteoli, U.; Antonaroli, S.; Marini, A.; Crociani, B. *Tetrahedron* **2005**, *61*, 9752−9758. Fluorous dba-type ligands stabilize Pd nanoparticles, see: (c) Moreno-Mañas, M.; Pleixats, R.; Villarroya, S. *Organometallics* **2001**, *20*, 4524−4528. (d) Moreno-Mañas, M.; Pleixats, R.; Villarroya, S. *Chem. Commun.* **2002**, 60−61. (e) Tristany, M.; Courmarcel, J.; Dieudonné, P.; Moreno-Mañas, M.; Pleixats, R.; Rimola, A.; Sodupe, M.; Villarroya, S. *Chem. Mater.* **2006**, *18*, 716−722.

(7) Breazzano, S. P.; Poudel, Y. B.; Boger, D. L. *J. Am. Chem. Soc.* **2013**, *135*, 1600−1606.

(8) Ueda, S.; Su, M.; Buchwald, S. L. *J. Am. Chem. Soc.* **2012**, *134*, 700−706.

(9) Zhang, H.-H.; Xing, C.-H.; Hu, Q.-S. J. *Am. Chem. Soc.* **2012**, *134*, 13156−13159.

(10) In our previous papers, see refs 5b and 11, we have referred to the aryl substituted dibenzylidene acetones as dba-*n,n′*-Z, which in this paper is simplified to dba-Z for symmetrical compounds.

(11) (a) Fairlamb, I. J. S.; Kapdi, A. R.; Lee, A. F. *Org. Lett.* **2004**, *6*, 4435−4438. (b) Macé, Y.; Kapdi, A. R.; Fairlamb, I. J. S.; Jutand, A. *Organometallics* **2006**, *25*, 1795−1800. (c) Fairlamb, I. J. S.; Kapdi, A. R.; Lee, A. F.; McGlacken, G. P.; Weissburger, F.; de Vries, A. H. M.; Schmieder-van de Vondervoort, L. *Chem.—Eur. J.* **2006**, *12*, 8750−8761. For related work with ionic chalcones, see: (d) Bäuerlein, P. S.; Fairlamb, I. J. S.; Jarvis, A. G.; Lee, A. F.; Müller, C.; Slattery, J. M.; Thatcher, R. J.; Vogt, D.; Whitwood, A. C. *Chem. Commun.* **2009**, 5734−5736.

(12) Fairlamb, I. J. S.; Lee, A. F. *Organometallics* **2007**, *26*, 4087−4089.
(13) (a) Zhao, Y.; Wang, H.; Hou, X.; Hu, Y.; Lei, A.; Zhang, H.; Zhu, L. *J. Am. Chem. Soc.* **2006**, *128*, 15048−15049. For related ligand effects, see: (b) Liu, Q.; Duan, H.; Luo, X.; Tang, Y.; Li, G.; Huang, R.; Lei, A. *Adv. Synth. Catal.* **2008**, *350*, 1349−1354. (c) Luo, X.; Zhang, H.; Duan, H.; Liu, Q.; Zhu, L.; Zhang, T.; Lei, A. *Org. Lett.* **2007**, *9*, 4571−4574. (d) Shi, W.; Luo, Y.; Luo, X.; Chao, L.; Zhang, H.; Wang, J.; Lei, A. *J. Am. Chem. Soc.* **2008**, *130*, 14713−14720.
(14) Firmansjah, L.; Fu, G. C. *J. Am. Chem. Soc.* **2007**, *129*, 11340−11341.
(15) (a) Denmark, S. E.; Werner, N. S *J. Am. Chem. Soc.* **2008**, *130*, 16382−16393. (b) Denmark, S. E.; Werner, N. S. *J. Am. Chem. Soc.* **2010**, *132*, 3612−3620.
(16) Sehnal, P.; Taghzouti, H.; Fairlamb, I. J. S.; Jutand, A.; Lee, A. F.; Whitwood, A. C. *Organometallics* **2009**, *28*, 824−829.
(17) Eddy, J. W.; Davey, E. A.; Malsom, R. D.; Ehle, A. R.; Kassel, S.; Goodson, F. E. *Macromolecules* **2009**, *42*, 8611−8614.
(18) Kawazura, H.; Tanaka, H.; Yamada, K.-i.; Takahashi, T.; Ishii, Y. *Bull. Chem. Soc. Jpn.* **1978**, *51*, 3466−3470.
(19) Tanaka, H.; Yamada, K.-i.; Kawazura, H. *J. Chem. Soc., Perkin Trans. II* **1978**, 231−235.
(20) Jarvis, A. G. PhD thesis, University of York, U.K., 2010.
(21) (a) Jarvis, A. G.; Whitwood, A. C.; Fairlamb, I. J. S. *Dalton Trans.* **2011**, *40*, 3695−3702. (b) Jarvis, A. G.; Sehnal, P. E.; Bajwa, S. E.; Whitwood, A. C.; Zhang, X.; Cheung, M. S.; Lin, Z.; Fairlamb, I. J. S. *Chem. Eur. J.* **2013**, *19*, 6034−6043.
(22) Zalesskiy, S. S.; Ananikov, V. P. *Organometallics* **2012**, *31*, 2302−2309.
(23) Preliminary data from our isotopic labeling study, highlighted herein, which showed the major and minor isomers of $Pd^0_2(dba)_3$ were reported (presented by Fairlamb, I. J. S.) at two separate international conferences: (a) ICOMC conference in Zaragoza, Spain in July 2006. (b) Canadian Chemical Society conference, Winnipeg, Canada in May 2007.
(24) Flash photolysis experiments on $Pd^0_2(dba)_3$, resulting in complex deactivation, have been reported, see: Hubig, M. S.; Drouin, M. A.; Michel, A.; Harvey, P. D. *Inorg. Chem.* **1992**, *31*, 5375−5380.
(25) (a) Pierpont, C. G.; Mazza, M. C. *Inorg. Chem.* **1974**, *13*, 1891−1895. (b) Mazza, M. C.; Pierpont, C. G. *J. Chem. Soc., Chem. Commun.* **1973**, 207−208.
(26) The X-ray structure of $Pd(dba)_3$·benzene has been determined: Mazza, M. C.; Pierpont, C. G. *Inorg. Chem.* **1973**, *12*, 2955−2959.
(27) Selvakumar, K.; Valentini, M.; Wörle, M.; Pregosin, P. S.; Albinati, A. *Organometallics* **1999**, *18*, 1207−1215.
(28) In Pregosin's structure of $Pd_2(dba)_3$·CH_2Cl_2 (ref 27) the phenyl groups in the different dba conformers were not differentiated, although excessive thermal disorder was seen.
(29) Zhao, H.; Ariafard, A.; Lin, Z. *Inorg. Chim. Acta* **2006**, *359*, 3527−3534.
(30) Takahashi, Y.; Ito, T.; Sakai, S.; Ishii, Y. *J. Chem. Soc., Dalton Trans.* **1970**, 1065−1066.
(31) Franzen, S. *J. Chem. Educ.* **2011**, *88*, 619−623 and references cited therein.
(32) (a) Franzen, S.; Cerruti, M.; Leonard, D. N.; Duscher, G. *J. Am. Chem. Soc.* **2007**, *129*, 15340−15346. (b) Leonard, D. N.; Cerruti, M.; Duscher, G.; Franzen, S. *Langmuir* **2008**, *24*, 7803−7809. (c) Leonard, D. N.; Franzen, S. *J. Phys. Chem. C* **2009**, *113*, 12706−12714.
(33) We did not characterize the Pd particles formed in the majority of these reactions, as one can observe them by the naked eye, indicating that they are large (>10 μm).
(34) Ukai, T.; Kawazura, H.; Ishii, Y.; Bonnet, J. J.; Ibers, J. A. *J. Organomet. Chem.* **1974**, *65*, 253−266.
(35) See ref 16 − from this previous work we used *procedure B* to access palladium complexes containing thienyl analogues of dibenzylideneacetone (dba), without issue.
(36) (a) Harvey, P. D.; Adar, F.; Gray, H. B. *J. Am. Chem. Soc.* **1989**, *111*, 1312−1315. (b) Hubig, S. M.; Drouin, M.; Michel, A.; Harvey, P. D. *Inorg. Chem.* **1992**, *31*, 5375−5380.
(37) SQUEEZE was used to correct for disordered solvent, as there appears to be a large void/channel in the center of the unit cell which may be a place for solvent to aggregate. While this is not an issue for the actual structure determination, it could affect the values of *R* and w*R*2.
(38) (a) Csaszar, P.; Pulay, P. *J. Mol. Struct.* **1984**, *114*, 31−34. (b) Ahlrichs, R.; Bar, M.; Haser, M.; Horn, H.; Kolmel, C. *Chem. Phys. Lett.* **1989**, *162*, 165−169. (c) Eichkorn, K.; Treutler, O.; Ohm, H.; Haser, M.; Ahlrichs, R. *Chem. Phys. Lett.* **1995**, *240*, 283−289. (d) Treutler, O.; Ahlrichs, R. *J. Chem. Phys.* **1995**, *102*, 346−354. (e) Eichkorn, K.; Weigend, F.; Treutler, O.; Ahlrichs, R. *Theo.Chem. Acc.* **1997**, *97*, 119−124. (f) Arnim, M. v.; Ahlrichs, R. *J. Chem. Phys.* **1999**, *111*, 9183−9190. (g) Deglmann, P.; Furche, F. *J. Chem. Phys.* **2002**, *117*, 9535−9538. (h) Deglmann, P.; Furche, F.; Ahlrichs, R. *Chem. Phys. Lett.* **2002**, *362*, 511−518. (i) Deglmann, P.; May, K.; Furche, F.; Ahlrichs, R. *Chem. Phys. Lett.* **2004**, *384*, 103−107.